NASA

Technical Memorandum **79701**

The Magnetic Field of Mercury

N. F. Ness

JANUARY 1979

National Aeronautics a.
Space Administration

Goddard Space Flight Center
Greenbelt, Maryland 20771

THE MAGNETIC FIELD OF MERCURY

N. F. Ness
Laboratory for Extraterrestrial Physics
NASA-Goddard Space Flight Center
Greenbelt, MD 20771

Presented at
The Conference on Origins of Planetary Magnetism
held in Houston, Texas 8-11 November 1978.
To be published in the proceedings.

THE MAGNETIC FIELD OF MERCURY

ABSTRACT

Direct observations of the magnetic field of Mercury and its magnetosphere, formed by the interaction of the solar wind, were performed twice by the Mariner 10 spacecraft, in March of 1974 and again in March 1975. From these data, it is clear that there exists an intrinsic magnetic field of the planet, sufficiently strong at present to deflect the solar wind flow around the planet and to form a detached bow shock wave in the super Alfvenic solar wind.

Four methods have been used to analyze the magnetic field data and derive quantitative values for the description of the planetary field:

1. Comparison of bow shock and magnetopause relative positions at Mercury to those at Earth,

2. Direct spherical harmonic analysis of the data,

3. Modeling of the magnetosphere by an image dipole and infinite 2-D current sheet in addition to the planetary field,

4. Scaling of a mathematical model for the terrestrial magnetosphere.

The results obtained yield dipole moments $\sqrt{(g_1^0)^2+(H_1^1)^2+(g_1^1)^2}$ ranging from 2.4 to 5.1×10^{22} gauss-cm^3, with the lower values associated with certain models using partial quadrupole (g_2^0) and octupole (g_3^0) terms to improve the least squares fitting of models to observations. Because the data set is incomplete, in the mathematical sense, no unique representation of the planetary field multipolar representation can be derived by method (2). The use of only 1 of the 5 quadrupole moment terms and 1 of the 8 octupole moment terms corresponds to a displacement of the dipole along its axis. These terms, used in

methods (3) and (4), yield equivalent offsets of the dipole by approximately 0.2 R_M. The selection of only those higher order terms possessing axial symmetry cannot be justified. Thus, the large offset may reflect the limitations of the models used to represent the external current systems. Because of the relatively short radial excursion of the data, the g_2^0 and g_3^0 terms can also be spatially aliased with the g_1^0 term.

Analyses by method (2) of subsets of data from the third encounter, taken near closest approach, yield a convergent series of dipole moment values which are believed to best represent the intrinsic planetary field. These provide a mean moment of $330(\pm 18)\gamma\ R_M^3 = 4.8 \times 10^{22}$ gauss-cm^3 at a tilt angle of $14^\circ \pm 5$ and a longitude of $148^\circ \pm 21^\circ$. This means that the surface field at Mercury is about 1% of Earth's, while the moment is 6×10^{-4} of Earth's. The polarity sense is the same.

The origin of the field cannot be uniquely determined. It may be due to an active dynamo, a remanent magnetic field or a combination. Consideration of remanence as the source leads to some difficulties, although definitive knowledge of the planetary interior structure and thermal state is lacking sufficient to absolutely eliminate this source. Success in attempting to explain the field as due to an active dynamo has encouraged these efforts. Therefore, Mercury may join Earth and Jupiter as an example of a planet possessing an internal fluid region with a convecting motion which regeneratively maintains the magnetic field. The source of convective energy may be radiogenic decay and heat release, gravitational settling and differentiation or precessional torques.

INTRODUCTION

Direct observations of the magnetic field of Mercury and its magnetosphere, as formed by the interaction of the solar wind, were made by the USA Mariner 10 spacecraft, in March of 1974 and again in March 1975 (Ness et al., 1974; Ness et al., 1975; Ness et al., 1976). From these data, it was discovered that there exists an intrinsic magnetic field of the planet Mercury, sufficiently strong at present to deflect the solar wind flow around the planet, thereby forming a well developed detached bow shock wave in the super-Alfvenic solar wind flow. Analyses of two other closely related experiments, the plasma and energetic particle instruments, have also appeared (Ogilvie et a., 1974; Hartle et al., 1975; Ogilvie et al., 1977 and Simpson et al., 1974). One unique aspect of the observations during the first encounter was the detection of a sudden change of the state of the magnetosphere, which was interpreted to be similar to that identified in the terrestrial magnetosphere as a substorm (Siscoe, Ness and Yeates, 1974).

It is the purpose of this paper to very briefly review the magnetic field observations and their analyses as they relate to the determination of the magnetic field of the planet. In addition, the implication of this magnetic field with respect to its origin within the planetary interior is considered from two model viewpoints; passive remanent magnetization or an active core dynamo. The existence of a magnetic field at Mercury provides the only firm experimental evidence that Mercury is a differentiated planet,

consistent with theoretical models of planetary evolution which predict that to be the case.

MAGNETIC FIELD OBSERVATIONS

Earlier publications have presented graphically the observations during the two encounters with Mercury by Mariner 10 as well as discussed their specific characteristics. Only a summary of salient features and some recent work extending the analyses is presented here. Figure 1 presents two views of the sub-Mariner 10 trace on the surface of the planet, while the spacecraft was located within its magnetosphere. Both close fly-bys occurred on the night-side of the planet and the third was especially selected to compliment the measurements and interpretations of data obtained from the first. The second encounter in September 1974 is not discussed in this paper because no direct observations of the magnetosphere or bow shock were possible since the spacecraft passed more than 50,000 km from the surface of the planet, in order to provide good imaging coverage of the south polar region.

Readily evident in Figure 1 is the contrast in the latitude region covered by the two fly-bys. The first was almost a pure equatorial pass, with a closest approach distance $R = 1.30\ R_M$ (planetocentric) while the second was almost a polar pass, with a closest approach distance of only $1.13\ R_M$.

The data obtained from these two encounters is shown in Figure 2, where the magnitude of the field, F, and the relative fluctuations, δ/F, are presented on logarithmic scales. Individual

data points were obtained at 25 Hz and component averaged over 6 second intervals, from which reconstructed vector field representations were obtained. Readily evident in this figure is the significant difference in the magnitudes of the field measured in the first and third encounters, as well as the magnitude of the relative fluctuations. The maximum field observed during the third encounter was 400 nT while that during the first encounter was only 100 nT, itself a factor of 4-5 times the interplanetary field strength. More important, notice should be made that following data point 90 of the first encounter, there is a significant increase in the relative fluctuations accompanied by a decrease in the magnetic field intensity. This signals the onset of the disturbance referred to earlier and already discussed as a Hermean substorm.

An important aspect to consider in the analysis and interpretation of these data, with respect to the intrinsic planetary magnetic field, is the relative contribution due to currents external to the planet which arise because of the deflected solar wind flow. Although specific measurements of the ion component of the solar wind plasma were not made by Mariner 10, measurements of the electron component of the plasma indicate differences in the momentum flux observed between the two encounters and the magnetic field observations also show differences in the interplanetary field.

Thus, with different "upstream" solar wind conditions, it would not be expected that the resulting external current patterns would be identical for the two sets of data. This creates a problem in

that one must choose which data set is most representative of a stationary magnetosphere. Clearly, the third encounter satisfies that requirement and carries with it the additional benefit that the average magnitudes measured during the third encounter were much larger than those during the first encounter. This is due partly to the fact that the average distance of third encounter measurements was 1.41 R_M as opposed to 1.76 R_M for the first encounter.

The distribution of field magnitude observed during the first and third encounters and the distribution of the radial distances of the spacecraft for the data sets I and III are shown in Figure 3. There is no question but that the two data sets are distincly different in the magnitude distribution, where it is seen that the median field magnitude for the third encounter (125 nT) is a factor of 2.5 times that of the median for the first encounter.

INTRINSIC FIELD ANALYSES

Four different methods have been used to analyze the observations and derive quantitative values for the description of the planetary magnetic field;

1. Comparison of bow shock and magnetopause positions relative to those observed at Earth;
2. Direct spherical harmonic analysis of the data;
3. Modelling of the magnetosphere by use of an image dipole and infinite current sheet in addition to the planetary field, and
4. Scaling of a mathematical model for the terrestrial magnetosphere.

The results obtained yield dipole moments, M, from 2.4 to 5.1×10^{22} gauss-cm^3, with equivalent equatorial field intensities of 165 - 350 nT. In terms of the individual gaussian coefficients the dipole moment is defined as

$$M = \sqrt{(g_1^0)^2 + (g_1^1)^2 + (h_1^1)^2}$$

The lower values of the dipole moment are associated with those studies using methods 3 and 4 and employing partial quadrupole (g_2^0) and octupole (g_3^0) terms to improve the least square fits of the model to the observations. In addition, users of methods 3 and 4 have included data from both encounter I and III, thus mixing the data sets and the external current systems.

The bow shock and magnetopause are located much closer to Mercury than at Earth, by a factor of 7.5, after normalizing by the planetary radius. This yields, along with the plasma observations of the momentum flux, an estimate of the equivalent dipole moment of $3\text{-}7 \times 10^{22}$ gauss-cm^3 by method 1.

The data set available for use of method 2 is incomplete, in the mathematical sense, because it does not provide vector measurements over a closed surface surrounding the planet. Such a spatial distribution of data is necessary in order to uniquely determine the separate contributions of magnetic fields due to sources internal to the planet and those external to the surface on which the measurements are performed. Thus, no unique determinations of the planetary magnetic field representation can be derived with method 2.

The use of only one of the five possible quadrupole moment terms and one of the eight possible octupole moment terms in methods 3 and 4 is arbitrary and can not be justified. The use of these terms corresponds to a displacement of the dipole along its axis given by the following relationship:

$$\Delta_Z = \frac{1}{2} \frac{g_2^0}{g_1^0}$$

It is well known that neither the Earth nor Jupiter (Acuna and Ness, 1976) show the axial symmetry of their planetary fields which would justify incorporation of only the g_2^0 and g_3^0 terms. Their inclusion, as used in methods 3 and 4 by Whang (1977), Jackson and Beard (1977) and Ng and Beard (1978) yield offsets of the dipole, $\Delta_Z = 0.2\ R_M$, where Z is parallel to the dipole axis.

A summary of all analyses of the planetary field at Mercury is presented in Table I. Included in the last entry are the results obtained in this paper and to be discussed shortly. Some of the differences in the dipole terms probably reflect the limitations of the models used to represent the external current systems and the confusion caused in the analyses by incorporating both data sets from the two encounters. In addition, it is also certain that because of the relatively short radial excursion of the data, the putative g_2^0 and g_3^0 terms are also spatially aliased with the g_1^0 term.

Recent analyses by method 2 of subsets of data from the third encounter taken near closest approach have shown a convergent series

of dipole moment values, which are believed to best represent the intrinsic planetary field. These results are shown in Figure 4, where a series of six successive solutions is shown for each model, classified by Im En. The value of m indicates the highest order of the internal terms while the value of n indicates the highest order of the external terms. Note that as the subset identification number increases from 1 to 6, the number of data points incorporated increases from 20 to 125. It is seen that for all three solutions I1E0, I1E1 and I1E2, using three different assumptions for the complexity of the external current system, the orientation of the dipole moment vector is well determined. The latitude is found to be $14^{o}\pm5^{o}$ while the longitude is $148^{o}\pm21^{o}$. The error bars graphically illustrate the orientation uncertainty in the main dipole moment term. Notice should be taken of the stability of the equatorial field intensity, which is 332 ± 4 nT for all three solutions, while the root mean squared deviation of the fits of the models to the data decreases substantially from 19 to 9.3 nT as n is increased.

An important consideration in the analysis of such data by least squares approximation is whether or not the analysis is well conditioned with respect to mathematical stability. A measure of this can be obtained by determining the condition number of the solution matrix. Figure 4 shows that the condition number increases from 2 to 519 as the order of the external field is increased. From experience, it is known that values of the condition number greater than 500 can lead to serious mathematical instabilities and

so no higher order approximations have been attempted.

The data intervals used in the individual data sets are illustrated in Figure 5, where the three components of the observations are shown compared to the IlEl model, previously published. Figure 5 also includes a measure of the relative contribution of external source fields to the observations in the upper most panel on the left hand side. There it is seen that, for most of the data, the principle contribution to the observations is due to the internal magnetic field. It is necessary to be cautious in any modelling process whereby one can improve a fit to a data set while invoking a physically implausible model. Such a case could be developed here if one increased the order of the external fields beyond n = 2.

As shown in Table I, those models which incorporate only a dipole term but use methods 3 and 4 provide dipole moments which are approximately 80% of the value obtained by direct spherical harmonic analysis. Considering the incorporation of the two encounter data sets and the differences caused by different solar wind conditions, this is felt to be reasonably good agreement. However, when those methods incorporate higher order specially selected quadrupole and octupole terms, there is a substantial decrease in the dipole moment subsequently determined. As previously discussed, this is felt to be an artifact of the analyses and not to reflect the true character of the planetary field.

INTERIOR OF MERCURY

A recent review of previous studies of the interior of Mercury

has been presented by Ness (1978). Here the results of those studies on the internal structure are summarized in Table II. The radius of the core formed during planetary evolution is seen to be quite large, approximately 0.75 of the planet itself, due to the large iron mass fraction, deduced by all investigators, 65%. The possible internal structure of the planet, as summarized in Table II, is based upon a number of assumptions about the conditions at the time of formation of the planet and its subsequent evolution. The existence of a planetary magnetic field argues strongly for a differentiated planet since at present it is believed that only an active dynamo or a passive remanent magnetic field can be the source of any planetary field. Another common feature of the thermal evolution models is that the sub Curie point depth is very close to the planetary surface so that only a thin lithospheric shell is available, if remanence is to be the source of the external field.

Table III summarizes the studies conducted on remanent magnetization as a possible source of the planetary field of Mercury, assuming the dipole moment of 330 nT $R_M^3 = 4.8 \times 10^{22}$ gauss-cm^3. All the thermal evolution models have led to lithospheric shells below the Curie point of only a few hundred kilometers thickness. Thus, the magnetization levels required, as shown in Table III, exceed significantly those observed in the average lunar sample magnetization. Thus, remanent magnetization does not appear to be a very plausible source of the magnetic field of Mercury.

Therefore, the possibility that an active dynamo must exist

at Mercury appears compelling. To examine this, we now consider current developments in dynamo theory, also reviewed at this conference. The most promising model which has been developed is that of Busse (1978), who invokes contiguous, cylindrical convection cells parallel to the axis of rotation of the planet. He has demonstrated their existence in his analogue model studies and has also mathematically attempted their analysis. Table IV summarizes the salient physical parameters for the three planets in the solar system known unequivocally to possess a magnetic field of internal origin. The important point in this brief summary of Busse's extensive work is that the upper bound on the relative magnetic energy density factor, $\lambda/K*M$, is approximately the same for all the three planets. Busse suggests, thusly, that his model has general applicability to the planets and the process of dynamo formation. It is inappropriate in this paper to review dynamo theory further and the reader is referenced to other articles in this conference proceedings for more extensive discussions by active participants in that field.

SUMMARY

As a result of unique observations by the USA Mariner 10 spacecraft in 1974 and 1975, Mercury has been discovered to possess a modest but significant intrinsic planetary field. Because the field is weak, the solar wind greatly distorts the planetary magnetic field as it forms a magnetosphere. Quantitative analyses indicate that the undistorted planetary field is primarily a dipole with its axis $14^{o}\pm5^{o}$ from the rotation axis of the planet and in the same sense

as Earth's. The undistorted equatorial field intensity is 330±18 nT yielding an equivalent dipole magnetic moment of 4.8×10^{22} gauss-cm^3.

The planet occupies an extremely large fraction of its magnetosphere, when compared to Earth. The average sub-solar point stagnation distance at the magnetopause is predicted to be 1.65±.15 R_M, a factor of 6 times smaller than at Earth's average position (10.4 R_E).

While thermo-remanent magnetization is a possible source of the intrinsic field, it requires an anomalously high percentage of free-iron in the anticipated thin sub-Curie point lithosphere and an extremely strong ancient dynamo. This alternative appears somewhat implausible at present, and a more likely source is an active dynamo. This requires a partially fluid core. This requirement is consistent with theoretical models of planetary evolution which have been put forward. Indeed, the existence of a planetary field argues convincingly that the planetary interior is differentiated, regardless of the source of the magnetic field.

Undoubtedly, remanent magnetic fields must exist on Mercury and when they are measured they may well provide an invaluable historical record of the formation of the planet. Whether or not they shall be as revealing as the studies of magnetic striping in the ocean bottoms, which led to the development of plate tectonic theory, is of course unknown at present. A very close orbiting spacecraft and/or a surface rover will be required in the future because the remanent fields may be so small.

REFERENCES

Acuna, M. H. and Ness, N. F., 1976. The main magnetic field of Jupiter, J. Geophys. Res., 81: 2917 - 2922.

Busse, F., 1978. Magnetohydrodynamics of the Earth's dynamo, Ann. Revs. Fluid Mech., 10: 435-462.

Hartle, R. E., Ogilvie, K. W., Scudder, J. D., Bridge, H. S., Siscoe, G. L., Lazarus, A. J., Vasyliunas, V. M., and Yeates, C. M., 1975. Preliminary interpretation of plasma electron observations at the third encounter of Mariner 10 with Mercury, Nature, 225: 206-208.

Jackson, D. J. and Beard, D. B., 1977. Magnetic field of Mercury, J. Geophys. Res., 82: 2828-2836.

Ness, N. F., Behannon, K. W., Lepping, R. P., Schatten, K. H., and Whang, Y. C., 1974. Magnetic field observations near Mercury: Preliminary results from Mariner 10, Science, 185: 151-160.

Ness, N. F., Behannon, K. W., Lepping, R. P., and Whang, Y. C., 1975. Magnetic field of Mercury: Part I, J. Geophys. Res., 80: 2708-2716.

Ness, N. F., Behannon, K. W., Lepping, R. P., and Whang, Y. C., 1976. Observations of Mercury's magnetic field, Icarus, 28: 479-488.

Ng, K. H. and Beard, D. B., 1978. Possible displacement of Mercury's dipole, preprint.

Ogilvie, K. W., Scudder, J. D., Hartle, R. E., Siscoe, G. L., Bridge, H. S., Lazarus, A. J., Asbridge, J. R., Bame, S. J., and Yeates, C. M., 1974. Observations of Mercury encounter

by the plasma science experiment on Mariner 10, Science, 185: 145-151.

Ogilvie, K. W., Scudder, J. D., Vasyliunas, V. M., Hartle, R. E., and Siscoe, G. L., 1977. Observations at the planet Mercury by the plasma electron experiment-Mariner 10, J. Geophys. Res., 82: 1807-1824.

Simpson, J. A., Eraker, J. H., Lamport, J. E., and Walpole, P. H., 1974. Electrons and protons accelerated in Mercury's magnetic field, Science, 185: 160-166.

Siscoe, G. L., Ness, N. F., and Yeates, C. M., 1974. Substorms on Mercury?, J. Geophys. Res., 80: 4359-4363.

Whang, Y. C., 1977. Magnetospheric magnetic field of Mercury. J. Geophys. Res., 82: 1024-1030.

ANALYSES OF INTRINSIC ☿ MAGNETIC FIELD*

SOURCE	DATA	g_1^0	g_2^0	g_3^0	EXTERNAL TERMS	OFFSET	TILT
NESS ET AL (1974)	I	227	0	0	NONE	$0.42R_M$	30°
NESS ET AL (1975)	I	350	0	0	SHC (n=2)	0	10°
NESS ET AL (1976)	III	342	0	0	SHC (n=1)	0	$11^\circ \pm 1^\circ$
WHANG (1977)	I	266	0	0	2-D TAIL SHEET	0	2.3°
	&	165	117	0	&	0	
	III	166	75	48	IMAGE DIPOLE	0	
JACKSON & BEARD (1977)	I	257	0	0	SCALED	0	10°-17°
	&				TERRESTRIAL		
	III	170	114	0	ANALOGUE	0	
NG & BEARD (1978)	I	190	0	0	(AS ABOVE)	(0.03,	1.2°
	&					0.03,	
	III					0.19)	
NESS (1978)	III	330 $\pm$18	0	0	SHC (n=2)	0	$14^\circ \pm 5^\circ$

(SHC = SPHERICAL HARMONIC COEFFICIENTS)

*USING DIPOLE ALIGNED COORDINATES ($g_n^m = h_n^m = 0$ FOR $n = 2,3$; $m = 1,2,3$)

TABLE I

INTERIOR OF MERCURY

KNOWN	ESTIMATED
$\bar{\rho}$ = 5.44 GMS/CC	$\rho(r,t_o)$ $T(r,t_o)$ $H(r,t_o)$
R = 2439 $\pm$ 1 KM	K(r,T) Cp(r,T)
$\tau_{ROT} = \frac{2}{3}\tau_{ORB}$ = 58.65 DAYS	f(DYNAMIC ELLIPTICITY)

AUTHOR	FE MASS FRACTION	CORE MF	CORE R_c/R	CORE C/MR^2
PLAGEMANN (1965)	-	0.77	0.86	-
KOZLOVSKAYA (1969)	0.588	0	0	0.368
	0.598	0.598	0.71	0.324
MAJEVA (1969)	0.58	0	0	-
REYNOLDS & SUMMERS (1969)	0.709	0	0	-
	0.675-0.687	0.681	0.79	-
SIEGFRIED & SOLOMON (1974)	0.69	0	0	0.394
	0.62	0.665	0.75	0.325
TOKSOZ & JOHNSTONE (1975)	-	-	0.69	-
SOLOMON (1976)	0.62	-	0.75	-
FRICKER ET AL. (1976)	0.66	-	0.78	-

TABLE II

THERMO-REMANENT MAGNETIZATION MODELS

AUTHOR	MODEL	SUB CURIE POINT CRUST & MANTLE THICKNESS (KM)	MAGNETIZATION (GAUSS CM^3/GM)	SURFACE POLAR FIELD (GAUSS)
NESS (1975)	UNIFORMLY MAGNETIZED	488	3.1×10^{-4}	
	SHELL	244	5.9×10^{-4}	
STEPHENSON (1976b)	ANCIENT DIPOLE	234	$C = 0.026p$	A) $\frac{2.4}{p}$
				B) $\frac{360}{p(1 - 3.6p)}$
STRANGWAY (1976)	UMS	100	1.8×10^{-3}	
SRNKA (1978)	ANCIENT DIPOLE	120	$C = 0.02$	B) 10.6 - 21.2
STEPHENSON (1976a)	AVERAGE LUNAR SAMPLE MAGNETIZATION		8×10^{-6}	

NOTES: $C = M_R/H$ = COEFFICIENT OF TRM ACQUISITION

A) FERROMAGNETIC INTERIOR

B) PARAMAGNETIC INTERIOR

p = % FREE IRON

TABLE III

PROPERTIES OF PLANETARY CORES - BUSSE (1978)

		EARTH	JUPITER	MERCURY
ANGULAR VELOCITY	$\Omega(10^{-5}\mathrm{SEC}^{-1})$	7.3	17.5	0.12
CHARACTERISTIC DIMENSION	$L(10^{6}\mathrm{m})$	3.5	10	1.8
MAGNETIC DIFFUSIVITY	$\lambda(\mathrm{m}^{2}\mathrm{sec}^{-1})$	1.6	1.2	1
THERMAL DIFFUSIVITY	$K(10^{-6}\mathrm{m}^{2}\mathrm{SEC}^{-1})$	7	40	4
MAGNETIC INDUCTION	$B(10^{-4}\ \mathrm{T})$	3.7	23	0.019
ENERGY DENSITY	$M(10^{-10})$	0.85	4.6	0.33
UPPER BOUND	$\frac{\lambda}{K}M(10^{-5})$	1.9	1.4	0.85

$\vec{B} = M^{1/2}\ (\vec{B}_0 + M\vec{B}_1 + \ldots)\ \vec{V} = \vec{V}_0 + M\vec{V}_1$

TABLE IV

FIGURE CAPTIONS

1. Two views of the trajectory of the Mariner 10 spacecraft as it transitted the Hermean magnetosphere in March 1974 and March 1975. The planetocentric distance at entry and exit from the magnetosphere is shown, as is the point of closest approach, identified by a + sign.
2. Magnetic observations obtained by the Mariner 10 spacecraft during the two transits through the magnetosphere described in Figure 1.
3. Statistical histograms of the field intensity and spatial position of the Mariner 10 spacecraft during the two encounters with the planet.
4. Summary of spherical harmonic analyses to determine the magnetic dipole moment of Mercury.
5. Comparison of observation and theory for analyses of the intrinsic planetary field during the Mariner 10 third encounter with Mercury. This figure illustrates the relative position of the six subsets of data selected for sequential analysis.

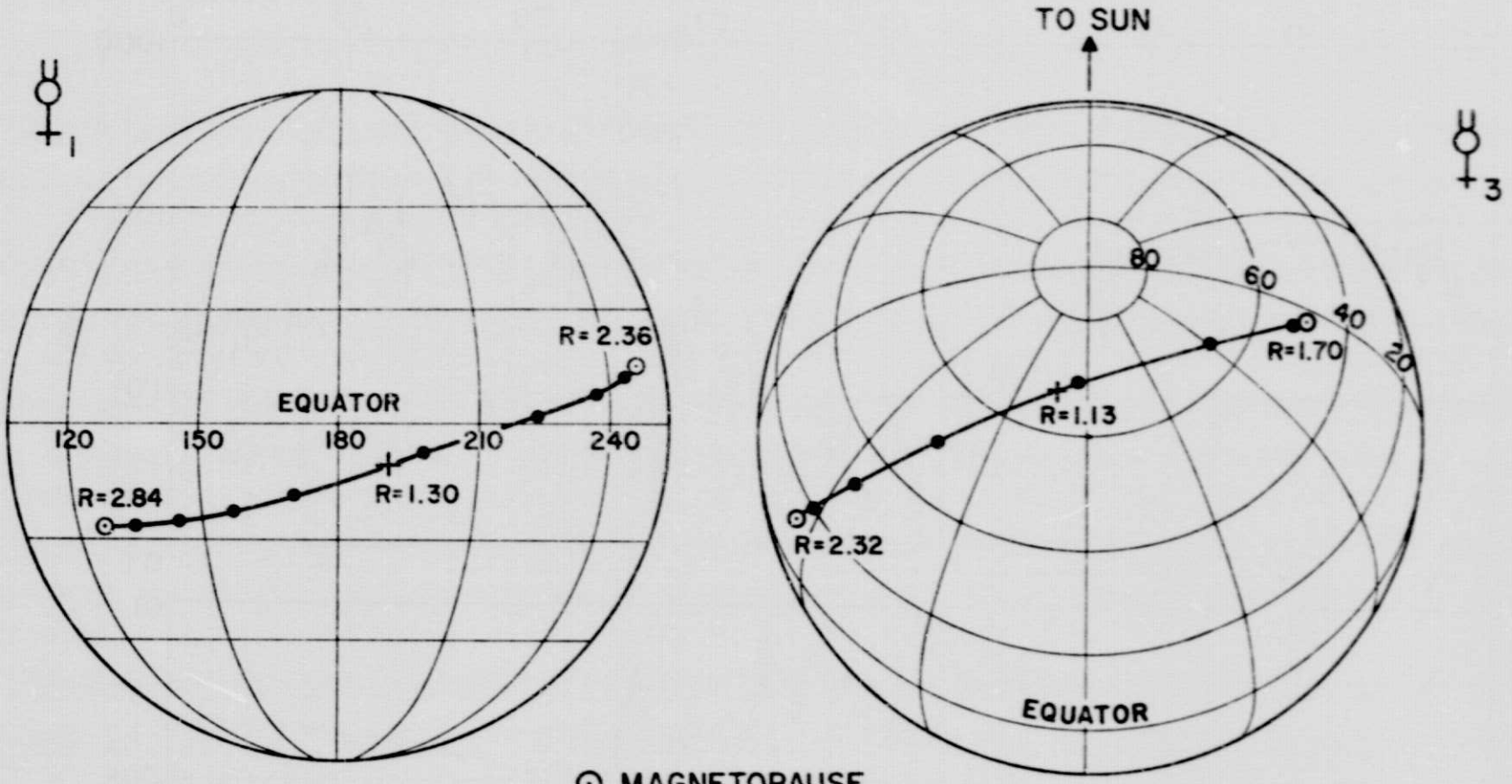

⊙ MAGNETOPAUSE
• ΔT = 2 MINUTES
+ CLOSEST APPROACH

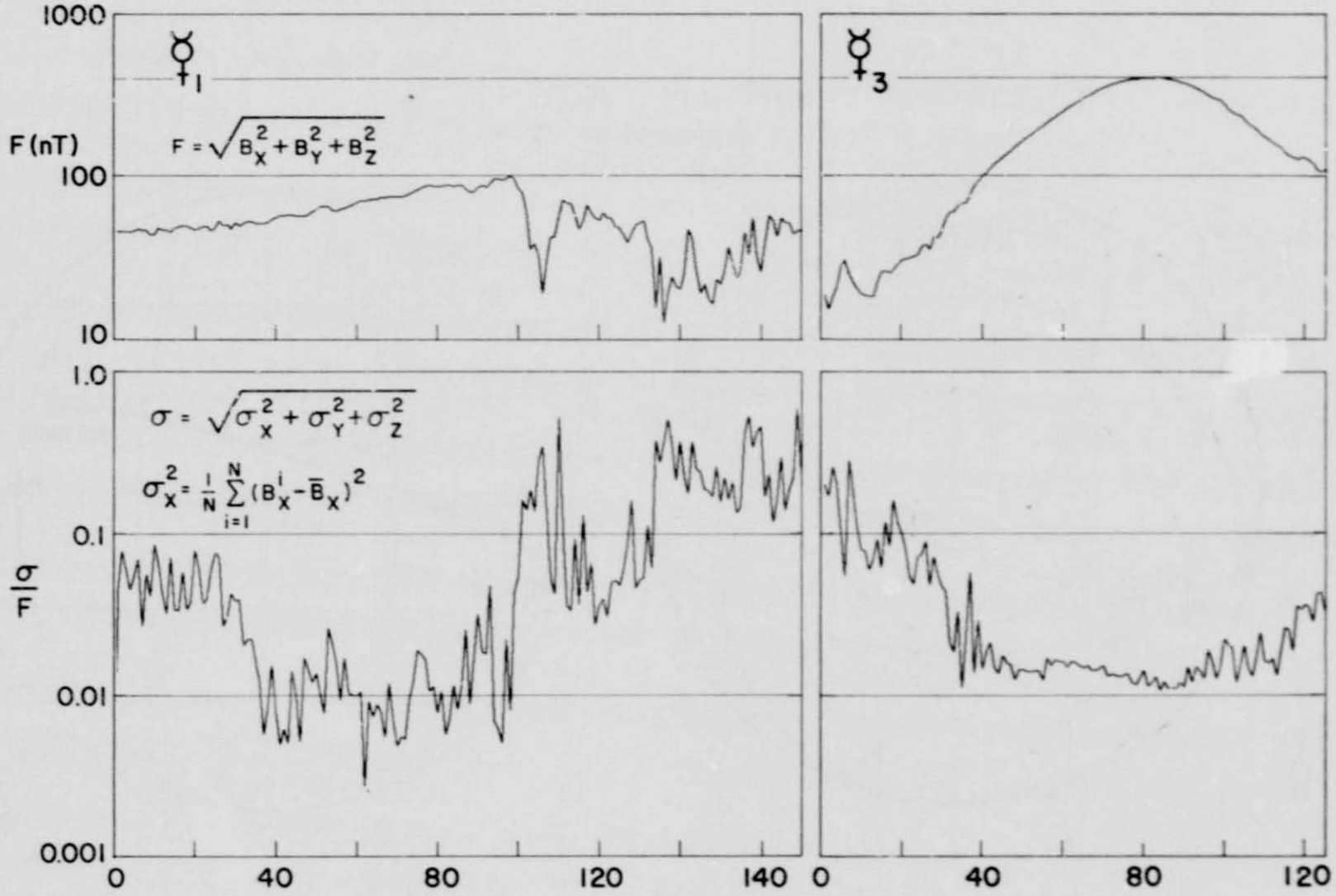
1000
100
10
F(nT)
☿1
☿3
$F = \sqrt{B_X^2 + B_Y^2 + B_Z^2}$
1.0
0.1
0.01
0.001
$\frac{\sigma}{F}$
$\sigma = \sqrt{\sigma_X^2 + \sigma_Y^2 + \sigma_Z^2}$
$\sigma_X^2 = \frac{1}{N}\sum_{i=1}^{N}(B_X^i - \bar{B}_X)^2$
0
40
80
120
140
0
40
80
120

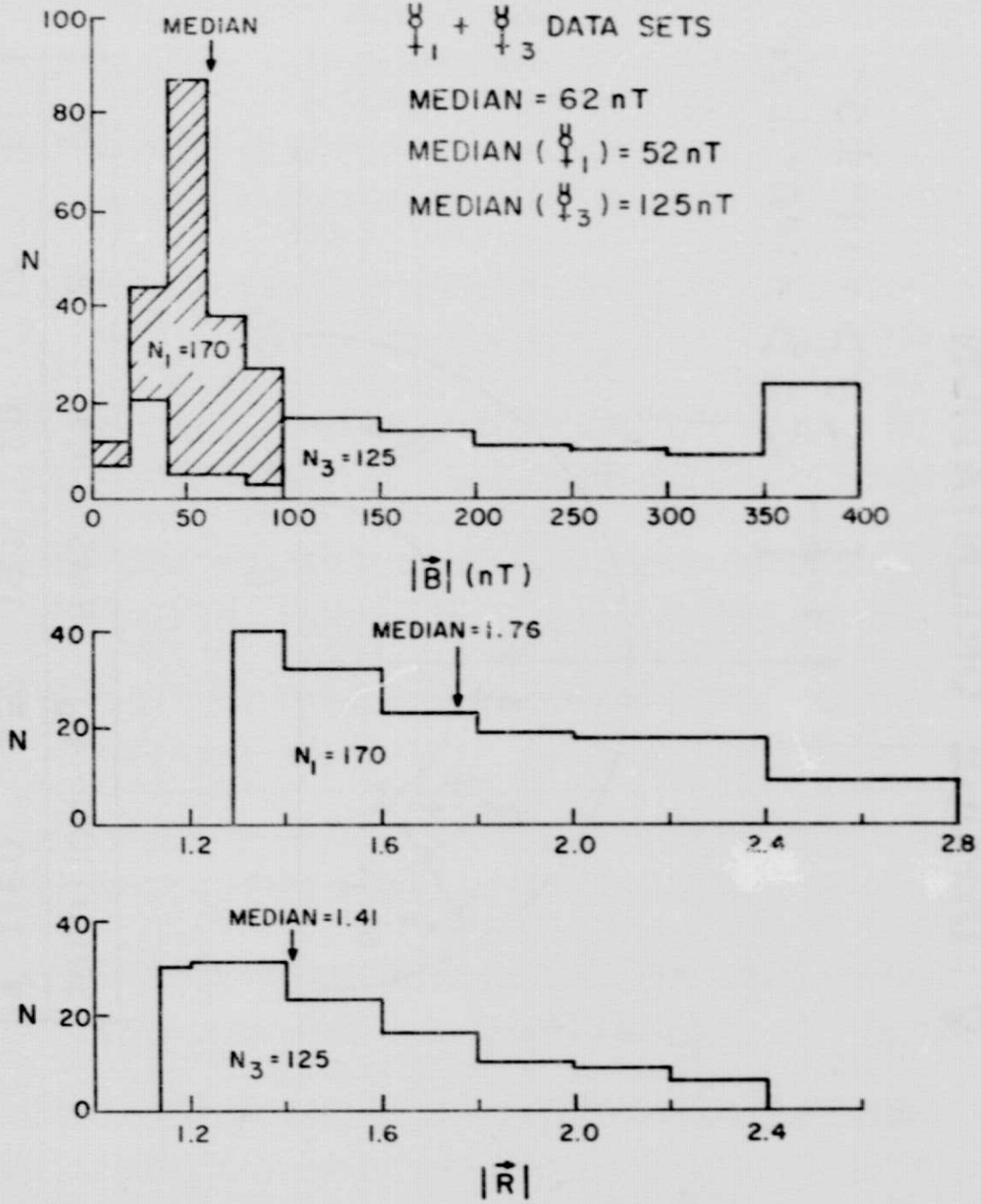
MEDIAN
♀1 + ♀3 DATA SETS
MEDIAN = 62 nT
MEDIAN (♀1) = 52 nT
MEDIAN (♀3) = 125 nT
N
N1 = 170
N3 = 125
|B| (nT)
MEDIAN = 1.76
MEDIAN = 1.41
|R|

CENTERED ☿ DIPOLE ORIENTATION

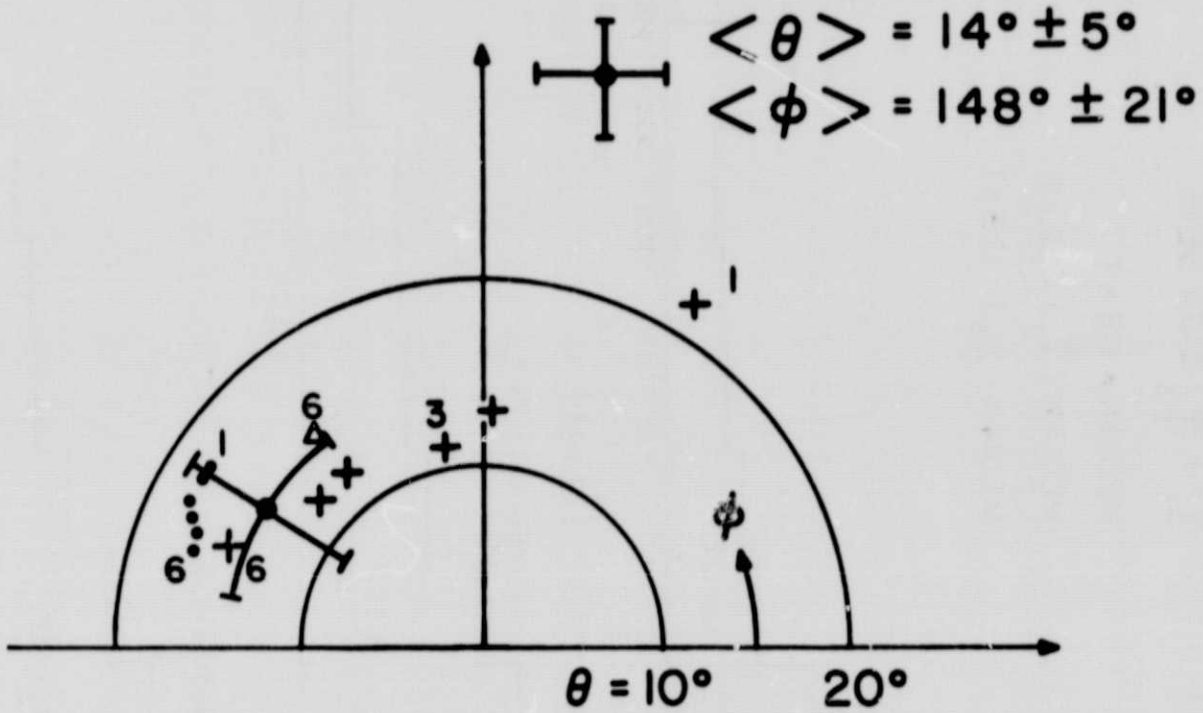

SOLUTION	B_0	RMS	CN	θ	φ
• I1E0	332	19.1	1.9	17	161
+ I1E1	328	18.6	6.3	15	158
△ I1E2	336	9.3	519	15	127

MERCURY III DATA SOLUTIONS (N=125)

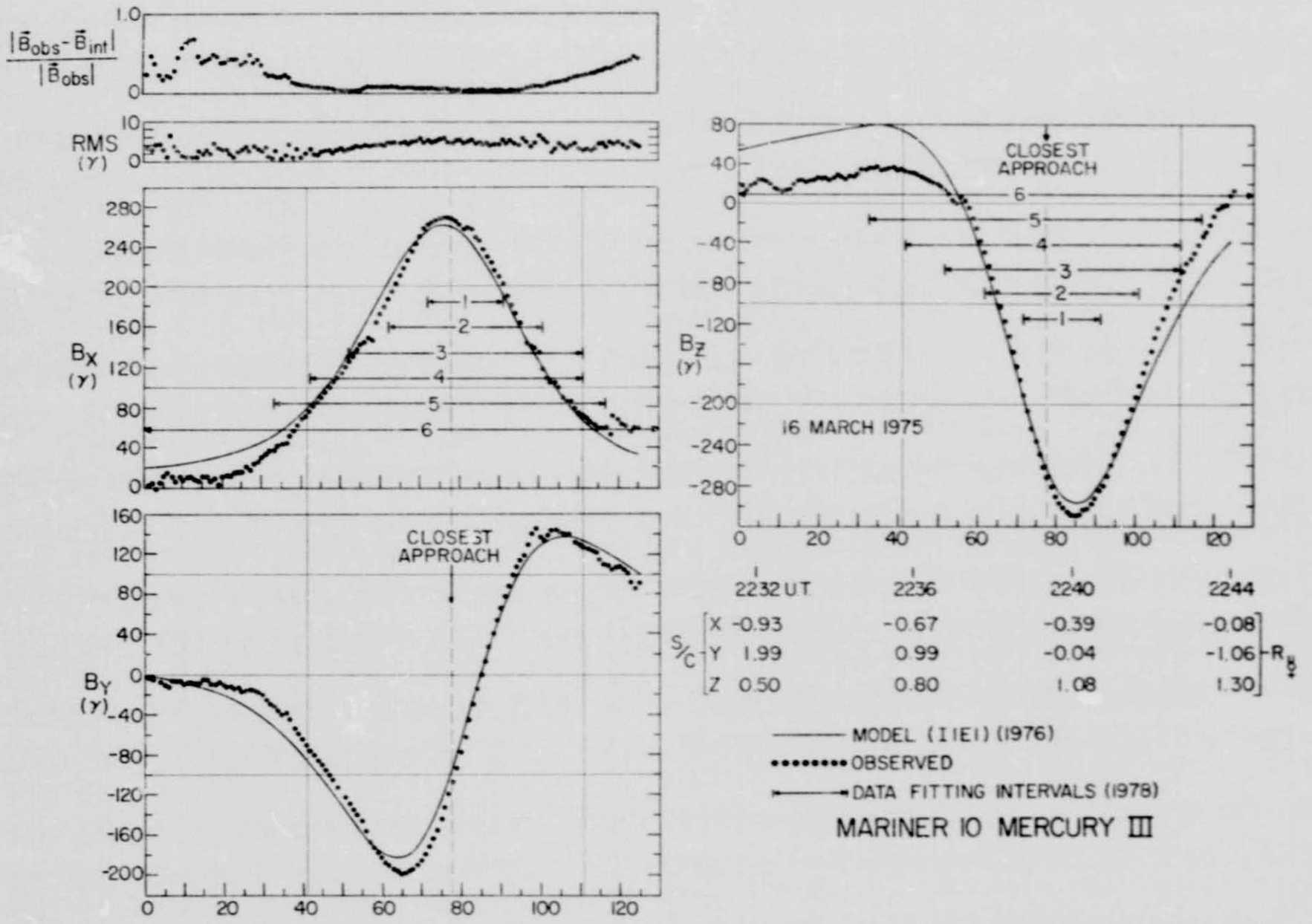
$\frac{|\vec{B}_{obs}-\vec{B}_{int}|}{|\vec{B}_{obs}|}$
1.0
0
RMS (γ)
10
0
B_X (γ)
280
240
200
160
120
80
40
0
1
2
3
4
5
6
CLOSEST APPROACH
B_Y (γ)
160
120
80
40
0
-40
-80
-120
-160
-200
0
20
40
60
80
100
120
B_Z (γ)
80
40
0
-40
-80
-120
-200
-240
-280
16 MARCH 1975
2232 UT
2236
2240
2244
S/C
X -0.93 -0.67 -0.39 -0.08
Y 1.99 0.99 -0.04 -1.06
Z 0.50 0.80 1.08 1.30
R_φ
MODEL (11E1) (1976)
OBSERVED
DATA FITTING INTERVALS (1978)
MARINER 10 MERCURY III